

Quantum wells and superlattices in strong time-dependent fields

Martin Holthaus

*Department of Physics and Center for Nonlinear Science,
University of California, Santa Barbara, Santa Barbara, California 93106*

Daniel Hone

*Department of Physics and Center for Quantized Electronic Structures,
University of California, Santa Barbara, Santa Barbara, California 93106*

(Received 24 August 1992)

The behavior of electrons in quantum semiconductor structures interacting with strong far-infrared laser radiation is discussed, under circumstances where quantum tunneling is important. The systematic appearance of avoided crossings in the quasienergy spectrum of a two-state system is related to the frequency spectrum of radiation scattered from a laser-driven double well. The application of the adiabatic approximation to a periodically forced superlattice explains the collapse of quasienergy minibands and leads to the prediction of a possible inhibition of wave-packet spreading.

I. INTRODUCTION

In the past two decades, enormous progress has been made in the field of quantum semiconductor structures.¹ In particular, using the technique of molecular-beam epitaxy, one can grow artificial layered structures made of, e.g., $\text{Al}_x\text{Ga}_{1-x}\text{As}$, with spatial modulation on an atomic scale of the concentration x so that the electrons can be confined by an almost arbitrary potential in the growth direction (though they remain essentially free in the plane perpendicular to that direction). Quantization within the potential well along the growth direction gives a discrete set of one-dimensional wave functions; associated with each is a “subband” of levels corresponding to all possible values of the wave vector in the perpendicular plane. For such a “quantum well” with typical width of a few hundred angstroms the intersubband energy spacings are of the order of tens of meV—in the far-infrared region. A powerful tunable far-infrared laser, such as the one available at the Center for Free Electron Laser Studies at UCSB, is therefore ideally suited to drive such a system.

As has been emphasized recently by Sherwin,² these developments have led to a new field of investigation spanning the areas of quantum optics and solid-state physics. Solid-state systems can now be used for the experimental study of the interaction of electrons with strong electromagnetic radiation. In particular, quantum wells exposed to far-infrared laser fields are promising candidates for a systematic investigation of nonperturbative phenomena.³

One can fabricate not only “solid-state atoms”² or isolated quantum wells, but also structures in which quantum tunneling is of crucial importance: double quantum wells or even superlattices—i.e., chains of such wells. It is the way in which these systems respond to strong time-periodic fields that we will discuss in this paper.

The low-lying levels of a double quantum well can be described approximately as a two-state system. Two-state dynamics, moreover, play a central role in under-

standing the behavior of more elaborate dynamical systems. Therefore, after briefly reviewing some mathematical tools in Sec. II, we study this system in Sec. III, with special emphasis on a systematic treatment of those effects which are beyond the scope of the familiar rotating-wave approximation. The central simplifying feature of a superlattice, on the other hand, is its approximate spatial periodicity. This allows us to apply the techniques of crystalline solid-state physics, including the introduction of Bloch states and the equivalent Hamiltonian approximation, to superlattices interacting with an external time-periodic force (Sec. IV). The paper closes in Sec. V with some concluding remarks.

II. MATHEMATICAL BACKGROUND

The Bloch theorem,⁴ which plays such a central role in the understanding of excitations in the spatially periodic crystals of solid-state physics, is a special case of a result enunciated earlier by Floquet.⁵ If a linear Hermitean operator \mathcal{L} , acting on functions of a variable s , is invariant under discrete translations by a of that variable, then the eigenfunctions of \mathcal{L} are of the form $e^{i\gamma s}u(s)$, with $u(s)$ periodic with the same period a : $u(s+a)=u(s)$. Where s is a spatial coordinate (for a crystalline solid) this gives as the electronic wave functions the usual Bloch states $\psi(x)=e^{ikx}u(x)$. The Floquet result is similarly applicable to systems with discrete time translational symmetry, such as those in which we are interested here, whose dynamics are governed by the time-dependent Schrödinger equation:

$$[\mathcal{H}(t)-i\partial_t]\psi=0, \quad (2.1)$$

with a time translationally symmetric Hamiltonian: $\mathcal{H}(t)=\mathcal{H}(t+T)$ (we have set Planck’s constant \hbar equal to unity). Then the eigenfunctions $\psi(t)$ are of the form $e^{-i\epsilon t}u(t)$, with $u(t+T)=u(t)$. Just as the wave vector k in the Bloch function is given the name “quasimomentum,” in recognition of its analogy to momentum under

the discrete translations of the symmetry group, rather than the continuous ones of free space, so ε is designated as a “quasienergy.”^{6,7} If the amplitude of the periodically varying part of the Hamiltonian (e.g., the strength of a time-periodic electric field) is regarded as an adjustable parameter, then ε becomes the energy as that amplitude vanishes. And in the same way that the Bloch states are conveniently labeled by the index k , plus a “band” index to distinguish between different states with the same quasimomentum, so the time-dependent solutions to the periodically driven system are conveniently labeled by the quasienergy ε . In analogy to the Bloch solutions for the spatially periodic situation, the quasienergy label is ambiguous within integral multiples of $\omega \equiv 2\pi/T$, the frequencies which make up arbitrary T -periodic functions of t :

$$\begin{aligned}\psi(t) &= e^{-i\varepsilon t} u(t) \\ &= e^{-i(\varepsilon+m\omega)t} e^{im\omega t} u(t) = e^{-i(\varepsilon+m\omega)t} \bar{u}(t),\end{aligned}\quad (2.2)$$

where $\bar{u}(t) = \bar{u}(t+T)$ whenever $u(t)$ has that same periodicity. Then by subtraction of a suitable integral multiple of ω the quasienergy can be restricted to the range $-\omega/2 < \varepsilon \leq \omega/2$, the first “Brillouin zone.”

Moreover, because the time-dependent Schrödinger equation is *first* order in the time derivative, in contrast to the spatial case, the quasienergies can be regarded as the eigenvalues of a stationary problem analogous to the time-independent Schrödinger equation:

$$[\mathcal{H}(t) - i\partial_t]u(t) = \varepsilon u(t), \quad (2.3)$$

with the time-periodic “Floquet functions” $u(t)$ playing the role of stationary states. These functions are defined within an extended Hilbert space of square integrable, T -periodic functions, with a scalar product

$$\langle\langle \cdot | \cdot \rangle\rangle = \frac{1}{T} \int_0^T dt \langle \cdot | \cdot \rangle. \quad (2.4)$$

As was first pointed out by Sambé,⁸ this direct analogy permits, among other things, the immediate translation of the complete formalism of stationary-state perturbation theory to the current problem. Of course, the matrix elements now must employ the scalar product defined by (2.4) and the “energy denominators” become differences between unperturbed quasienergy values.

We will examine the functional dependence of the quasienergies on the strength of the applied periodic external field (of fixed frequency). Then as the field strength is varied adiabatically (as it is physically with typical laser pulses), one expects the system to evolve through a set of time-dependent Floquet states described by the calculated functional dependence of ε on the field amplitude. In the common situation when the number of energy eigenstates in the absence of a periodic field is infinite, this picture is complicated somewhat by the denseness of the quasienergy spectrum within the reduced zone scheme.⁹ The set of eigenvalues from all “bands” then, in general, fills the first zone densely, but the weakness of the connection between states from well-separated zones (or, mathematically speaking, the low degree of spectral concentration at a particular quasienergy) still makes this a useful picture.

III. THE TWO-STATE SYSTEM

A particularly simple system for analysis, which is also of great practical importance, is one in which there are only two important energy eigenstates in the absence of the T -periodic potential. This is effectively the case, e.g., for a single pair of quantum wells, when the lowest-energy pair of states, split by tunneling between the wells, is separated from the next pair by an amount much greater than all other relevant energies, including the tunnel splitting, Hamiltonian matrix elements (the field strength must not be too large), and the periodic frequency, $\omega = 2\pi/T$. Within that two-state space the Hamiltonian describing the interaction with a linearly polarized sinusoidal electric field of frequency ω can be written as

$$\mathcal{H}(t) = (\omega_0/2)\sigma_z + \sigma_x \lambda \cos(\omega t), \quad (3.1)$$

where σ_x and σ_z are the usual Pauli matrices. Note that the level separation ω_0 is a superfluous parameter, in that it only sets the overall energy scale, and we will choose dimensionless units with ω_0 equal in unity in the numerical examples below. This Hamiltonian has been well studied,^{10,11} not only in connection with the nonlinear response of atomic systems to lasers¹² but also, e.g., for the magnetic resonance of spins $\frac{1}{2}$ (Ref. 13) and for the radiation of pions from fast nucleons passing through nuclear matter.¹⁴ It is instructive for the problems in which we are interested here to examine its behavior in terms of the associated quasienergy spectrum as a function of coupling constant λ for different frequencies ω .

As is well known, the Schrödinger equation (2.1) with the Hamiltonian (3.1) cannot be integrated in closed form, essentially because $\mathcal{H}(t)$ does not commute with itself at different times: $[\mathcal{H}(t), \mathcal{H}(t')] \neq 0$ (since the Pauli matrices do not commute with one another: $[\sigma_x, \sigma_z] = -2i\sigma_y$). Nevertheless, we will see that we can understand the important features of numerical solutions to the problem from suitable simple analytic approximations.

For a numerical solution it is convenient to introduce the usual time-evolution operator $U(t, t')$ by $\psi(t) = U(t, t')\psi(t')$, or as the 2×2 matrix,

$$\begin{aligned}U_{n',n}(t, t') &= \langle n'(t) | n(t') \rangle \\ &= \langle n'(0) | U(t, t') | n(0) \rangle.\end{aligned}\quad (3.2)$$

From the Bloch form (2.2) of the solution to the Schrödinger equation (2.1) we have immediately that in the basis of those solutions $U_{n',n}(T, 0)$ is diagonal, with eigenvalues $e^{-i\varepsilon T}$, where T is again the period. Thus, using the initial condition $U(0, 0) = I$, the identity operator, we numerically integrate the equation $i\partial_t U(t, 0) = \mathcal{H}(t)U(t, 0)$ over one period and diagonalize $U(T, 0)$ to obtain the quasienergies ε . The results are shown in Fig. 1 for $\omega = 2\pi/T = 0.23$, and in Fig. 2 for $\omega = 0.18$; in both case we take units so that the level separation $\omega_0 = 1$.

For an analytic approach we make use of the insights to be gained from an approximate reduction to a time-independent problem, the familiar “rotating-wave approximation.”¹⁵ The physical idea is perhaps clearest

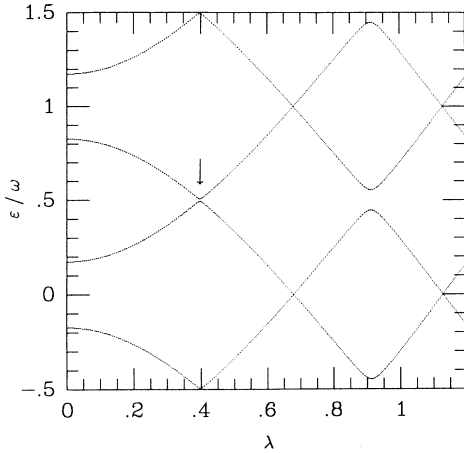


FIG. 1. Two Brillouin zones of quasienergies (in units of ω) for the driven two-level system (3.1) as functions of the coupling strength λ for $\omega_0=1$ and $\omega=0.23$. Note that there are no crossings at the zone boundaries. The first “gap,” indicated by the arrow, is an avoided crossing with $N=4$ that appears in second-order perturbation theory (cf. Fig. 3); the second one is a third-order effect ($N=6$; see Fig. 4). In this and the following figures the quasienergies are given in the laboratory frame; rotating-frame values are simply shifted by $\omega/2$ from these.

within the magnetic resonance interpretation of (3.1). If the “magnetic field” $\lambda \cos(\omega t)$, linearly polarized along x , is decomposed into two fields oppositely circularly polarized along the z axis, then by transforming to a frame of reference rotating with one of these we reduce it to a static field. The other field, now rotating with twice the original frequency, 2ω , can then often be treated perturbatively. Thus we rewrite (3.1) as

$$\mathcal{H}(t) = \frac{\omega_0}{2} \sigma_z + \frac{\lambda}{2} \{ [\sigma_x \cos(\omega t) + \sigma_y \sin(\omega t)] + [\sigma_x \cos(\omega t) - \sigma_y \sin(\omega t)] \}. \quad (3.3)$$

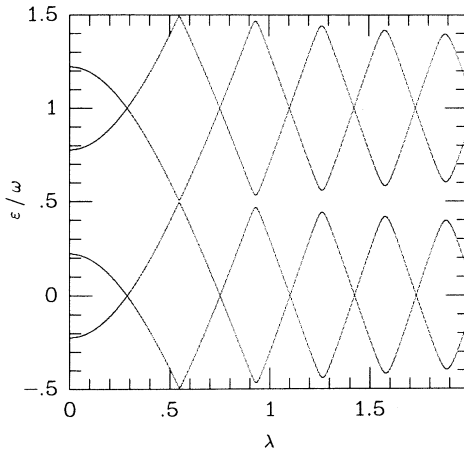


FIG. 2. Two Brillouin zones of quasienergies (in units of ω) for the driven two-level system (3.1) as functions of the coupling strength λ for $\omega_0=1$ and $\omega=0.18$. The avoided crossing at $\lambda \approx 0.55$ appears in third-order perturbation theory ($N=6$; see Fig. 5).

A unitary transformation to the frame rotating about the z axis with frequency ω then gives

$$\begin{aligned} e^{i\omega t \sigma_z / 2} [\mathcal{H}(t) - i\partial_t] e^{-i\omega t \sigma_z / 2} &= \frac{(\omega_0 - \omega) \sigma_z + \lambda \sigma_x}{2} \\ &+ \frac{\lambda}{2} [\sigma_x \cos(2\omega t) - \sigma_y \sin(2\omega t)] - i\partial_t \\ &= \mathcal{H}'_{\text{RWA}} + \mathcal{H}'_{\text{CR}}(t) - i\partial_t, \end{aligned} \quad (3.4)$$

where the subscripts refer to “rotating-wave approximation” (the static piece) and “counter-rotating” (the explicitly time-dependent piece at frequency 2ω), and the superscript r denotes operators in the rotating frame. The solutions to the eigenvalue equation in that frame,

$$(\mathcal{H}' - i\partial_t) u^r(t) = (\epsilon \pm \omega/2) u^r(t) \equiv \epsilon' u^r(t), \quad (3.5)$$

are trivial, if we keep only the static part $\mathcal{H}'_{\text{RWA}}$ of the Hamiltonian: the spin aligns either parallel or antiparallel to the static field [z component $(\omega_0 - \omega)$ and x component λ]. Therefore, it is convenient to choose as axes in this frame one (which we label ξ) which is parallel to the static field; as the second we take the y axis at time $t=0$, relabeled η ; the third is labeled ξ . Then we have

$$\begin{aligned} \mathcal{H}'(t) = \frac{\Omega}{2} \sigma_\xi + \frac{\lambda}{2\Omega} \{ [(\omega_0 - \omega) \sigma_\xi + \lambda \sigma_\xi] \cos(2\omega t) \\ - \Omega \sigma_\eta \sin(2\omega t) \}, \end{aligned} \quad (3.6)$$

where

$$\Omega^2 = (\omega_0 - \omega)^2 + \lambda^2. \quad (3.7)$$

If we neglect the counter-rotating field,¹⁶ the time-evolution operator in this frame takes the simple form $U'_{\text{RWA}}(t, 0) = \exp(-i\sigma_\xi \Omega t / 2)$, and the Floquet states and quasienergy eigenvalues are

$$\psi'_+(t) = e^{-i\Omega t / 2} \begin{bmatrix} 1 \\ 0 \end{bmatrix}, \quad \psi'_-(t) = e^{+i\Omega t / 2} \begin{bmatrix} 0 \\ 1 \end{bmatrix}, \quad (3.8)$$

$$\epsilon'_\pm = \pm \Omega / 2 \text{ mod } \omega. \quad (3.9)$$

The standard formalism of Rayleigh-Schrödinger perturbation theory can now be used, with $\mathcal{H}'_{\text{CR}}(t)$ as the interaction Hamiltonian and the ϵ^r as the relevant “energies.” Because the scalar product (2.4) is integrated over a single period T , the complete set of basis states for expansion must include separately all values of ϵ^r differing by multiples of the frequency ω , i.e., the states in all the “Brillouin zones.” [Notice that the Hamiltonian in the rotating frame (3.6) is actually $T/2$ periodic. However, in order not to lose the one-to-one correspondence between Floquet states in the laboratory frame and the rotating frame, we continue to work in a space of T -periodic functions.] We label the state with quasienergy $\epsilon'_+ = \Omega/2 + M\omega$ by $(+, M)$ and that with quasienergy $\epsilon'_- = -\Omega/2 + N\omega$ by $(-, N)$, with M and N arbitrary integers, so that the periodic parts of the wave functions are

$$|+, M\rangle = \begin{pmatrix} 1 \\ 0 \end{pmatrix} e^{iM\omega t}, \quad |-, N\rangle = \begin{pmatrix} 0 \\ 1 \end{pmatrix} e^{iN\omega t}. \quad (3.10)$$

Within the rotating-wave approximation, there are two different types of quasienergy crossings. The equation $\Omega/2 + M\omega = -\Omega/2 + N\omega$ shows that a crossing occurs at $\varepsilon^r = 0 \pmod{\omega}$ if $(N - M)$ is even; if $(N - M)$ is odd, the quasienergies cross at $\varepsilon^r = \omega/2 \pmod{\omega}$. Note from (3.5) that the relation is reversed for the quasienergies ε in the lab, or nonrotating frame: the crossings for even and odd $(N - M)$ are, respectively, at the boundary and center of the Brillouin zone. For fundamental reasons of symmetry¹⁷ these two types of crossings behave very differently under the influence of the counter-rotating field. This is most easily seen in the rotating frame, where the approximate RWA Hamiltonian is time independent. This continuous time translational invariance, which allows both types of quasienergy crossings, is broken by the counter-rotating field, but not completely; the full Hamiltonian (3.6) is still invariant under time translations by $T/2$, half the laboratory period. Moreover, it is easy to see that the states (3.10) have parities $(-1)^M$ and $(-1)^N$ under this translation. If the approximate quasienergies cross in the center of the (lab frame) Brillouin zone, then the difference $(N - M)$ is odd, so that the corresponding RWA states have opposite parities. But in the case of a crossing at the zone boundary, the parity of the two states is the same. Thus, the degeneracies at the center of the Brillouin zone will persist even for the full Hamiltonian (3.6), but those at the zone boundaries will be lifted and turned into anticrossings. Figures 1 and 2 illustrate the effect clearly. It is this splitting of a quasienergy degeneracy, and its experimental relevance for quantum double-well structures in strong laser fields, that we will now study in more detail.

To this end, we will make use of nearly degenerate perturbation theory and try to understand the numerical results from an analytic point of view; the quantitative agreement will turn out to be remarkably good. We start from the observation that degeneracies at the Brillouin-zone boundaries occur for $\Omega = (N - M)\omega$, where $(N - M)$ is even. Since the perturbation \mathcal{H}'_{CR} contains only the frequencies $\pm 2\omega$, the degenerate unperturbed states are first connected in order $(N - M)/2$. The matrix elements are

$$\begin{aligned} \langle\langle +, M | \mathcal{H}'_{CR} | -, N \rangle\rangle &= \frac{\lambda}{4\Omega} \{ (\Omega + \omega_0 - \omega) \delta_{N-M, -2} \\ &\quad - [\Omega - (\omega_0 - \omega)] \delta_{N-M, +2} \}, \\ \langle\langle +, M | \mathcal{H}'_{CR} | +, N \rangle\rangle &= \frac{\lambda^2}{4\Omega} (\delta_{N-M, -2} + \delta_{N-M, +2}) \\ &= -\langle\langle -, M | \mathcal{H}'_{CR} | -, N \rangle\rangle. \end{aligned} \quad (3.11)$$

Note that only the *difference* $(N - M)$ of the integers characterizing the two states enters the expressions for the matrix elements. Thus, without loss of generality we can restrict ourselves to $M = 0$. In the simplest case we have $N = 2$ —that is, $\Omega/2 = -\Omega/2 + 2\omega$, or $\Omega = 2\omega$ for some external field strength λ . Then near that field amplitude we must diagonalize the Hamiltonian projected onto the space spanned by the two nearly degenerate states $(+, 0)$ and $(-, 2)$:

$$P\mathcal{H}^r = \begin{pmatrix} \Omega/2 & -\gamma \\ -\gamma & -\Omega/2 + 2\omega \end{pmatrix}, \quad (3.12)$$

where P is the projection operator onto the subspace and $\gamma = \lambda[\Omega - (\omega_0 - \omega)]/(4\Omega)$. Thus, in either the rotating reference frame or in the laboratory frame, a quasienergy gap of size 2γ is opened at the value of λ where the unperturbed quasienergies cross. In the neighborhood of the avoided crossing at $\Omega = 2\omega$ the quasienergies are given by

$$\varepsilon_{\pm}^r = \pm \frac{1}{2} \sqrt{(\Omega - 2\omega)^2 + 4\gamma^2} \pmod{\omega}. \quad (3.13)$$

If the degeneracy occurs for $N = 4$, so that $\Omega = 4\omega$ for a given field strength λ , we must consider the second-order perturbation Hamiltonian within the corresponding (nearly) degenerate subspace:

$$\begin{aligned} \langle\langle +, 0 | \mathcal{H}_{CR}^{(2)} | -, 4 \rangle\rangle &= \sum_{\sigma = +, -} \frac{\langle\langle +, 0 | \mathcal{H}'_{CR} | \sigma, 2 \rangle\rangle \langle\langle \sigma, 2 | \mathcal{H}'_{CR} | -, 4 \rangle\rangle}{\varepsilon_{-, 4}^r - \varepsilon_{\sigma, 2}^r} \\ &= \left[\frac{\lambda^3}{32\Omega} \right] \frac{\Omega - (\omega_0 - \omega)}{\omega(\Omega - 2\omega)} \equiv B. \end{aligned} \quad (3.14)$$

There are now also diagonal matrix elements within the nearly degenerate subspace:

$$\begin{aligned} \langle\langle +, 0 | \mathcal{H}_{CR}^{(2)} | +, 0 \rangle\rangle &= -\langle\langle -, 4 | \mathcal{H}_{CR}^{(2)} | -, 4 \rangle\rangle = \sum_{\mu = \pm 2} \frac{|\langle\langle +, 0 | \mathcal{H}'_{CR} | -, \mu \rangle\rangle|^2}{\Omega - \mu\omega} \\ &= \frac{\lambda^2}{8\Omega(\Omega^2 - 4\omega^2)} [\Omega^2 + (\omega_0 - \omega)^2 - 4\omega(\omega_0 - \omega)] \equiv A. \end{aligned} \quad (3.15)$$

(Note that the contributions from the two other channels $|+, 0\rangle \rightarrow |+, \pm 2\rangle \rightarrow |+, 0\rangle$ cancel each other.)

Thus the Hamiltonian within this subspace has the simple structure

$$P_{(2)}\mathcal{H}^r = \begin{pmatrix} \Omega/2 + A & B \\ B & -\Omega/2 + 4\omega - A \end{pmatrix}, \quad (3.16)$$

where A and B are the matrix elements given explicitly in (3.14) and (3.15). Again the quasienergies are given within nearly degenerate perturbation theory by the eigenvalues of this matrix:

$$\varepsilon_{\pm}^r = \pm \sqrt{(\Omega/2 - 2\omega + A)^2 + B^2} \pmod{\omega}. \quad (3.17)$$

For the first numerical example ($\omega = 0.23$; see Fig. 1) we

use this approximation in the neighborhood of the RWA degeneracy at $\Omega = 4\omega$, or $\lambda \approx 0.5$. As shown in Fig. 3, the low-order theory does very well in explaining both the location (shifted substantially from the unperturbed value) and the magnitude of the quasienergy gap.

For crossings with higher values of the "photon index" N , $\Omega = N\omega$ with $N > 4$ (and even), the degenerate states are connected to each other only in third or higher order (in fact, in order $N/2$) of the perturbation. However, as shown explicitly in (3.15), there is a diagonal term, or quasienergy shift, in every even order starting with the second. In the simplest case, $N=6$, the near degeneracy occurs at the value of λ for which $\Omega = 6\omega - 2A$ [with A given by (3.15)]. Then the third-order perturbation in the nearly degenerate subspace in the neighborhood of this point has the form

$$P_{(3)}\mathcal{H}^r = \begin{bmatrix} \Omega/2 - 3\omega + A & C \\ C & -\Omega/2 + 3\omega - A \end{bmatrix}, \quad (3.18)$$

where

$$C = \left[\frac{-\lambda^5}{512\Omega} \right] \frac{\Omega - (\omega_0 - \omega)}{\omega^2(\Omega - 2\omega)(\Omega - 4\omega)}, \quad (3.19)$$

and we have shifted the origin of quasienergy to place the degeneracy at $\epsilon^r = 0$. The quasienergies in the neighborhood of the resulting anticrossing are given within this lowest-order correction by

$$\epsilon_{\pm}^r = \pm \sqrt{(\Omega/2 - 3\omega + A)^2 + C^2} \text{ mod } \omega. \quad (3.20)$$

This result applies to the second anticrossing seen in Fig. 1. As shown in detail in Fig. 4, the predicted location of the gap is about right, whereas its size is clearly overestimated. But that should not be too surprising, since the RWA degeneracy occurs only at a relatively large value of the coupling strength, $\lambda \approx 1.14$, and one has to consider the fact that the perturbation matrix elements are

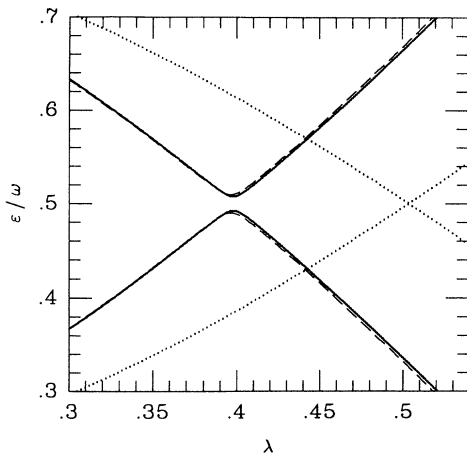


FIG. 3. Magnification of the first avoided crossing seen in Fig. 1. Full line, exact (numerically computed) quasienergies; dots, rotating-wave approximation; dashes, second-order degenerate perturbation theory. (For $\lambda < 0.4$, the exact and the perturbative results are almost identical.)

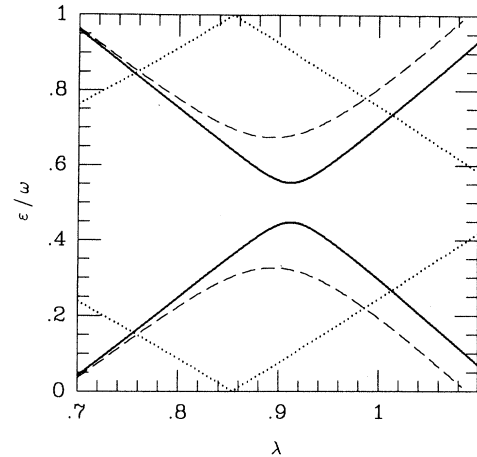


FIG. 4. Magnification of the second avoided crossing seen in Fig. 1. Full line, exact (numerically computed) quasienergies; dots, rotating-wave approximation; dashes, third-order degenerate perturbation theory.

comparable to, rather than much smaller than, the quasienergy denominators (so that one is suspicious about the potential convergence of the perturbation theory). A more favorable case for the application of perturbative techniques is the first avoided crossing of Fig. 2. In this example, the agreement of the third-order approximation with the numerical data is excellent (see Fig. 5).

In passing, we remark that the rotating-wave approximation is usually applied close to resonance, $\omega \approx \omega_0$. The present analysis shows that, in combination with perturbation theory for Floquet states, it can also serve as a good starting point for an analytical understanding of the low-frequency regime, where $\omega < \omega_0$.

These techniques not only give remarkably clear insight into the quasienergy spectrum of a two-level system

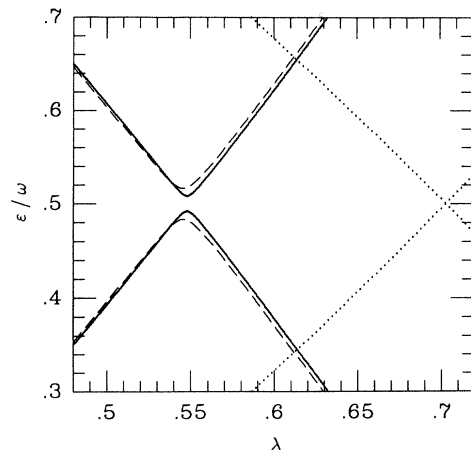


FIG. 5. Magnification of the first avoided crossing seen in Fig. 2. Full line, exact (numerically calculated) quasienergies; dots, rotating-wave approximation; dashes, third-order degenerate perturbation theory.

in a time-periodic electric field, but they also predict an interesting observable effect. As we have already pointed out, a possible experimental realization of a two-state system arises in the context of quantum semiconductor structures.¹ In the case of a symmetric $\text{Al}_x\text{Ga}_{1-x}\text{As}$ double quantum well, the energy ω_0 is given by the tunnel splitting of the two lowest states; it is typically of the order of a few meV. The dynamics of such a double well driven by intense monochromatic far-infrared radiation can be probed by measuring the spectrum of the emitted radiation. Under conditions where the rotating-wave approximation is valid (well away from anticrossings), the wave function can be written as a linear combination of the basis solutions (3.8):

$$\psi^r(t) = \begin{bmatrix} a_+ \\ 0 \end{bmatrix} e^{-i\Omega t/2} + \begin{bmatrix} 0 \\ a_- \end{bmatrix} e^{i\Omega t/2}, \quad (3.21)$$

where a_{\pm} are constant coefficients (notice that the indices N, M drop out of the physical wave function). It is then easy to verify that the time Fourier transform of the expectation value of the electric dipole moment (in the rotating frame) $\langle \psi^r(t) | \mu | \psi^r(t) \rangle$ contains only the frequencies $0, \Omega$; in the laboratory frame these are shifted by $\pm\omega$ to give frequencies $\omega, (\omega + \Omega)$, and $(\omega - \Omega)$, the well-known Mollow triplet.¹⁸

But this simple pattern changes when different rotating-wave Floquet states are strongly mixed by the counter-rotating Hamiltonian, in the neighborhood of an avoided crossing. For example, in the simplest case, where $|+, 0\rangle$ and $|-, 2\rangle$ become degenerate within the RWA, the proper Floquet states at the field strength λ of the RWA degeneracy are, in the rotating frame,

$$u_{\pm}^r(t) = \frac{1}{\sqrt{2}} (|+, 0\rangle \mp |-, 2\rangle), \quad (3.22)$$

with quasienergy eigenvalues $\varepsilon_{\pm}^r \approx \omega \pm \gamma$ [see (3.12)], so the complete wave function is $\psi^r(t) \approx a_+ u_+^r(t) e^{-i(\omega + \gamma)t} + a_- u_-^r(t) e^{-i(\omega - \gamma)t}$. Then the time-dependent dipole moment contains the frequencies $0, 2\omega, 2\gamma, 2(\omega + \gamma)$, and $2(\omega - \gamma)$ in the rotating frame, or $\omega, 3\omega, (\omega \pm 2\gamma)$, and $(3\omega \pm 2\gamma)$ in the laboratory frame. Similarly, an avoided crossing that emerges in higher order ($\Omega = N\omega$, with $N = 4, 6, \dots$) leads to a dipole with laboratory frame frequencies $m\omega, (m\omega + 2\gamma)$, and $(m\omega - 2\gamma)$, where $m = 1, (N - 1)$, or $(N + 1)$, and 2γ denotes the quasienergy splitting.

Thus, the occurrence of an avoided quasienergy crossing due to the breaking of a continuous symmetry by the counter-rotating field has a characteristic experimental signature: if one measures the frequency spectrum of the radiation emitted by a laser-driven double well at a field strength slightly lower than the “critical” field strength of an avoided crossing, one should obtain a comparatively simple spectrum. At the critical field strength the spectrum becomes significantly richer (depending on the order $N/2$ in which the anticrossing is generated), but it becomes simple again when the field strength is increased further. In principle, such an effect could, e.g., be used to determine the actual strength of the laser field that is coupled into the double-well heterostructure.

IV. SUPERLATTICES

A different example for the physics of semiconductor structures interacting with time-dependent fields emerges if, instead of a double quantum well, we consider a regular array of a large number of identical wells, i.e., a “superlattice.”¹⁹ If the number of wells is sufficiently large (or—at least in principle—if the wells are effectively arranged around a ring), the approximation of perfect lattice periodicity (in one dimension) can be made. Moreover, as a practical matter the wavelength of far-infrared laser radiation is long compared to the total length of the physical superlattice (a few thousand angstroms), so the spatial dependence of the electric field can be neglected. Then the single particle quantum states²⁰ are characterized not only by a quasienergy ε due to the periodicity in time of the external laser field, but also, because of the spatial periodicity, by a quasimomentum $\hbar k$ (note: in this section we explicitly include Planck’s constant \hbar in all expressions). In the parameter regime of interest we can neglect interband effects and describe the states in terms of independent bands, as follows.

If $\varphi_{nk}(x) = e^{ikx} u_{nk}(x)$ is a Bloch wave solution, in band n with wave vector k and energy $E_n(k)$, of the time-independent Schrödinger equation in the absence of an external field, then the periodic piece $u_{nk}(x)$ obeys the eigenvalue equation

$$\begin{aligned} [(p + \hbar k)^2 / 2m^* + V(x)] u_{nk}(x) \\ \equiv \mathcal{H}_k u_{nk}(x) = E_n(k) u_{nk}(x), \end{aligned} \quad (4.1)$$

where m^* is the effective mass for electrons in the semiconductor (approximately the same in the wells as in the barriers separating the wells). We will be interested in wave vectors k of order the inverse superlattice spacing, very small compared to inverse atomic separations, so this effective-mass approximation to the electron dynamics associated with the atomic periodic potential in the neighborhood of the conduction-band minimum is fully adequate. Then $V(x)$ is the smooth potential describing the spatial variation of the conduction-band minimum. This equivalent or effective-mass Hamiltonian approximation to the electron dynamics in a crystal with a potential slowly varying on an atomic scale is a familiar and well-established one²¹ in solid-state physics.

It is convenient to describe the time-dependent electric field in a transverse gauge: $c\mathcal{E}(t) = -dA(t)/dt$, with $A(t)$ the vector potential, which is introduced into the Schrödinger equation via the usual replacement $p \rightarrow p - eA(t)/c$. The justification for doing this within the effective-mass Hamiltonian is not trivial. For a static magnetic field it has been demonstrated²² that the replacement is the lowest-order modification within a systematic expansion scheme, and as is commonly done, we will assume it to be a valid procedure here. Because the vector potential does not depend on x , the wave vector k remains a good quantum number, and the full time-dependent wave functions $\psi_{nk}(x, t) = e^{ikx} v_{nk}(x, t)$ are determined by the equation

$$i\hbar \partial_t v_{nk}(x, t) = \mathcal{H}_{q(t)} v_{nk}(x, t), \quad (4.2)$$

where

$$q(t) \equiv k - eA(t)/\hbar c. \quad (4.3)$$

For the parameters of interest here we can invoke the adiabatic approximation to solve (4.2). Because the external field is homogeneous, the Hamiltonian connects only states of the same k in different bands. The individual bandwidths are set by the tunneling rate between wells and are therefore very small compared to interband separations, $E_n(k) - E_{n'}(k) \approx \hbar^2/m^*a^2$ (a is the lattice param-

eter of the superlattice), for any value of the wave vector k . For applied frequencies $\omega \ll \Delta/\hbar$, where Δ is an interband energy, this requires the change in Hamiltonian matrix elements during the period \hbar/Δ to be small compared to Δ . With momentum matrix elements of order \hbar/a , the condition is $e\mathcal{E}a \ll \Delta$, well satisfied²³ for typical values of the systems we are discussing: electric-field amplitudes of a few kV/cm, superlattice spacings a of order 100 Å, and $(m^*/m_e) \approx 0.1$ (and therefore interband energies Δ of order 50–100 meV). Then the standard adiabatic result²⁴ for (4.2) is the set of solutions

$$e^{-ikx}\psi_{nk}(x,t) = v_{nk}(x,t) = u_{nq(t)}(x) \exp \left\{ -\frac{i}{\hbar} \int_0^t d\tau E_n[k - eA(\tau)/\hbar c] \right\}. \quad (4.4)$$

[The phase at each time is set uniquely by the choice of $u_{nk}(x)$ as real, always possible in one dimension, so that $u_{nq(t)}(x)$ is orthogonal to its time derivative.²⁴] Although the wave vector k , describing the eigenvalue of discrete translations, is a constant in the present gauge, the label of the spatially periodic part of the wave function, or that of the adiabatically varying energy $E_n[q(t)]$, obeys the familiar force equation $\hbar\dot{q}(t) = e\mathcal{E}(t)$. Because $q(t)$ is a periodic function of time, it is now simple to write the wave functions $\psi_{nk}(x,t)$ explicitly as spatio-temporal Bloch waves which are characterized simultaneously by k and by a quasienergy ε_{nk} ,

$$\psi_{nk}(x,t) = e^{i(kx - \varepsilon_{nk}t/\hbar)} w_{nk}(x,t), \quad (4.5)$$

with a function $w_{nk}(x,t)$ that is periodic in both space and time, $w_{nk}(x,t) = w_{nk}(x+a,t) = w_{nk}(x,t+T)$:

$$\varepsilon_{nk} = \frac{1}{T} \int_0^T d\tau E_n[k - eA(\tau)/\hbar c], \quad (4.6)$$

$$w_{nk}(x,t) = \exp \left\{ -\frac{i}{\hbar} \int_0^t d\tau \{ E_n[k - eA(\tau)/\hbar c] - \varepsilon_{nk} \} \right\} u_{nq(t)}(x). \quad (4.7)$$

For a sinusoidal homogeneous electric field, $\mathcal{E}(t) = \mathcal{E}_0 \cos \omega t$, we have $A(t) = (-\mathcal{E}_0 c/\omega) \sin \omega t$. If, moreover, the band n is described approximately by a cosine dispersion relation, as is commonly the case (and the result of the standard nearest-neighbor tight-binding approximation that seems highly appropriate to this set of wells weakly coupled through tunneling barriers): $E_n(k) = E_{0n} - (W_n/2) \cos ka$, then (4.6) gives the simple expression

$$\varepsilon_{nk} = E_{0n} - (W_n/2)(\cos ka) J_0(e\mathcal{E}_0 a/\hbar\omega), \quad (4.8)$$

where $J_0(z)$ is the zeroth-order Bessel function.

The most obvious remarkable feature of this result is the degeneracy of the eigenvalues ε_{nk} simultaneously for *all* values of the wave vector k at values of the field strength (or of the frequency) given by the zeros of the Bessel function. One way of interpreting this physically is to look at the behavior of a wave packet driven by the sinusoidal electric field. It is one of the advantages of the present approach that arbitrary wave packets can be constructed from the Bloch waves (4.5) with constant coefficients a_k :

$$\psi(x,t) = \sum_k a_k e^{ikx} w_{nk}(x,t) e^{-i\varepsilon_{nk}t/\hbar}. \quad (4.9)$$

After one period, $t = T$, the periodic functions w_{nk} return

to their initial values, but in general they are weighted by different phase factors $\exp(-i\varepsilon_{nk}T/\hbar)$, and an initially localized wave packet has spread. However, at points of quasienergy degeneracy (at the special values of the field amplitude and frequency where the Bessel function vanishes, so that ε_{nk} is independent of k), all phase factors are equal, and the wave packets returns periodically to its initial spatial position *with its initial width*. At the zeros of J_0 , wave packets are in that sense similar to the “coherent” states of standard forced linear harmonic-oscillator theory, which follow classical phase-space trajectories as wave packets of constant minimum uncertainty width. In the present case the wave packet “breathes” while undergoing forced oscillations of its center, but it does not spread indefinitely with passing time, as it does for other values of the driving field parameters. [Though it is at first tempting to surmise, we note that these special points of quasienergy degeneracy are *not* those where the excursion of the wave packet covers exactly one, or a larger integral number l , of full Brillouin zones in k space. In this case, we have $\hbar\delta k = \int_0^{T/4} dt e\mathcal{E}(t) = l\pi\hbar/a$, which does occur simultaneously for all initial positions of the wave-packet center but at $e\mathcal{E}_0 a/(\hbar\omega) = l\pi$, rather than at the zeros of J_0 .]

This total degeneracy depends sensitively on the assumption of a cosine form of the dispersion relation. If,

for example, we include second-neighbor overlaps in the tight-binding model, which adds a term proportional to $\cos(2ka)$ to the $\cos(ka)$ term in the dispersion relation $E_n(k)$, then the quasienergies (4.6) will contain an additional term proportional to $\cos(2ka)J_0(2e\mathcal{E}_0a/\hbar\omega)$, and there is no value of the field strength \mathcal{E}_0 for which the full expression will vanish simultaneously for all wave vectors k [there are no mutual zeros of $J_0(z)$ and $J_0(2z)$].

By making one further common approximation we can make contact with the equivalent Hamiltonian approximation,²¹ for the *superlattice*, which introduces some additional simplicity, and which will be valuable for dealing with potentials which break the superlattice periodicity, including impurities and other imperfections. The dependence of the periodic functions $u_{nk}(x)$ on the wave vector k is often weak within a band n ; this is certainly the case in the tight-binding limit appropriate to the problems here. If we take these functions to be independent of k within the band, then we have from (4.4) as the adiabatic wave functions a linear combination of Bloch states $\varphi_{nk}(x) = u_n(x)e^{ikx}$ from that band:

$$\psi_{nk}(x, t) = \varphi_{nk}(x) \exp \left\{ -\frac{i}{\hbar} \int_0^t d\tau E_n[k - eA(\tau)/\hbar c] \right\}, \quad (4.10)$$

which obeys the simple dynamical equation (also often referred to as the “effective-mass equation”):

$$\{E_n[p - eA(t)/\hbar c] - i\hbar\partial_t\}\psi = 0. \quad (4.11)$$

We note that, with this simplification, the dynamical localization of wave packets at the special fields where quasienergies throughout the band are degenerate [at the zeros of the Bessel functions in (4.8)] can be applied directly to the localized Wannier states $W_n(x - la) \equiv \sum_k \exp(-ikla)\varphi_{nk}(x)$. An electron initially prepared in such a Wannier state will be found in the same localized state after an integral number of field periods T .

At this point, there is a close connection with the work of Dunlap and Kenkre,²⁵ who have recognized the possibility of dynamical localization of electrons in a tight-binding band. The present results provide a simple interpretation of this phenomenon. A necessary condition for this type of localization is that the width of the quasienergy band vanish, because only then is there no dephasing of the individual components that build up the wave packet (4.9). But in contrast to the time-independent case, a vanishing quasienergy bandwidth does not imply that a wave packet initially localized at a particular site remains localized there at all times. During one cycle, it can spread and/or tunnel to neighboring sites, and it reassembles itself (up to an irrelevant overall phase factor) only after integral multiples of the period T . A similar situation was discussed recently by Grossmann *et al.*²⁶ for an electron placed in a periodically driven symmetric double well, where the “bands” consist of just two states. If the wave function can be approximated by a linear combination of the two lowest Floquet states, these two components remain in phase at the points

where their quasienergies cross (see Sec. III), and an electron placed initially in one side of the well is found there again after any integral number of periods. But as with the spatially periodic case, the quasienergy degeneracy does not necessarily lead to localization in that side of the well at intermediate times.

In the discussion up to now, we have neglected both (i) interband effects: the influence of other than a single independent band, and (ii) departures from perfect spatial periodicity. The first of these is insignificant for the regime of parameters in which we are interested, as we suggested above, and as is verified by numerical calculations. The spatial periodicity is inevitably broken in real superlattices, first because the total number of wells is finite (and relatively small as a practical matter—perhaps of order 20 or so), and second because (in contrast to atomic systems) the successive wells are not identical to each other in size, shape, and separation; fabrication is always somewhat imperfect. Even if we neglect the breakdown of translational symmetry within the plane of the well (from well surface roughness, etc.), so that the dynamics remain effectively one dimensional, we must recognize that the wave vector k will no longer be an exact quantum number, and to that extent different states within the quasienergy Brillouin zone will be mixed by the perturbation and degeneracies will be lifted (there will be anticrossings). In particular, there will no longer be total quasienergy degeneracy at the zeros of J_0 . It is, therefore, essential to investigate the role of translational symmetry breaking. To this end, we compute the quasienergies for a finite chain of identical wells numerically; the wave functions are required to vanish at the ends of the chain.²⁷ As an example, we display in Fig. 6 two Brillouin zones of quasienergies for a chain with 20 square wells as functions of $y = e\mathcal{E}_0a/(\hbar\omega)$. The parameters for the numerical calculation were $a = 140 \text{ \AA}$ (well width 100 \AA , barrier width 40 \AA , barrier height 0.3 eV), $\hbar\omega = 2.0$

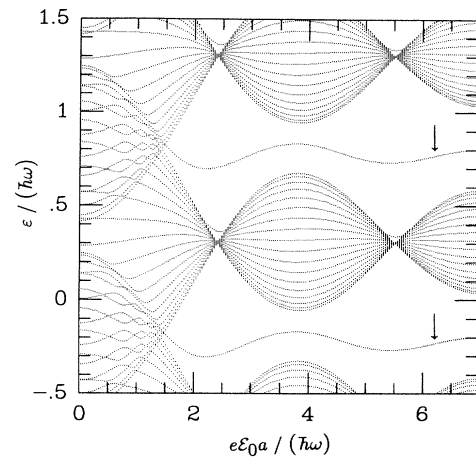


FIG. 6. Two Brillouin zones of quasienergies for the lowest miniband of a finite chain of 20 quantum wells with lattice constant a which interacts with a monochromatic force of strength \mathcal{E}_0 and frequency ω (see the text for the values of these parameters), plotted vs $y = e\mathcal{E}_0a/(\hbar\omega)$. The arrows indicate edge states.

meV, and an effective mass of $m^* = 0.066m_e$ was assumed. As in the preceding section, the frequency was fixed, and the electric-field strength \mathcal{E}_0 was varied. In this calculation only a single level per well (split by tunneling into a single miniband of width $W = 3.66$ meV for the whole chain) was retained. First of all, it is obvious that the overall agreement with (4.8) is quite good: The quasienergy miniband “collapses” precisely at $y = 2.405$ and 5.520 , the first two zeros of J_0 , although the finite boundary conditions necessarily imply that the collapse is imperfect.²⁸ In such a situation, the wave packets will be accurately, but not perfectly, coherent, so that the spreading of an initially localized packet can be slowed significantly, but not suppressed completely. There are two additional obvious finite-size effects: (i) a pair of almost degenerate states (indicated by the arrows), which physically are edge states spatially localized near the ends of the chain of wells, show markedly different quasienergy behavior from the others; they do not participate in the collapse, and (ii) there are avoided crossings. Since $\hbar\omega < W$, the miniband does not fit into a single quasienergy Brillouin zone at low \mathcal{E}_0 , and different “copies” (distinguished in quasienergy by integer multiples of the photon energy $\hbar\omega$) have to overlap. The appearance of avoided quasienergy crossings in the regions of self-overlap is a consequence of the fact that for this finite model k is only an approximate quantum number. Whereas the avoided crossings discussed in the preceding section resulted from the breaking of the rotating-wave symmetry (continuous time translational invariance, or time independence, in the rotating frame) by the counter-rotating field, those under consideration here result from the breaking of the exact discrete spatial translational symmetry. But the boundary conditions have only a relatively minor effect on the principal features of the spectrum.

The same thing cannot be said for the wave functions. The probability densities of spatio-temporal Bloch states (4.5) for the infinite periodically driven system are, of course, periodic in space with the lattice period a , but a computation of the Floquet states for the finite model^{27,28} shows that their probability densities do not share this feature. The phenomenon encountered here is analogous to that discussed by Rabinovitch and Zak²⁹ for electrons in a finite-range electric field. While the quasienergy spectrum is relatively insensitive to the boundary conditions, the eigenfunctions are strongly affected.

Again, from the experimental point of view, a way of probing the quasienergy spectrum (that is, of “quasienergy spectroscopy”) of a far-infrared driven superlattice is to measure the frequency spectrum of the emitted radiation. In analogy to (3.21), the wave function can be written as

$$\psi(x, t) = \sum_l a_l u_l(x, t) \exp(-i\varepsilon_l t / \hbar), \quad (4.12)$$

where the index l labels the states in the lowest miniband, and the $u_l(x, t)$ are the periodically time dependent (but, because of finite chain length, not spatially periodic) Floquet wave functions. If the parameter $y = e\mathcal{E}_0 a / (\hbar\omega)$ is chosen, say, at a local maximum of the Bessel function J_0 , the time Fourier transform of the mean dipole moment $\langle \psi(t) | \mu | \psi(t) \rangle$ obviously contains many different frequencies, corresponding to transitions between different miniband states. But if y becomes equal to a zero of J_0 (and if edge states are neglected), so that all ε_l are (almost) equal, the only possible frequencies of emitted radiation are integer multiples of $\hbar\omega$. Thus, the behavior of miniband quasienergies as shown in Fig. 6 should leave its signature in the spectrum of scattered radiation. We emphasize that there is an important difference from the semiclassical result,³⁰ which predicts that at the zeros of J_0 there should be no radiation at all.

V. CONCLUSION

We have outlined two possible schemes for using suitably designed quantum semiconductor structures for the study of the interaction of strong laser fields with matter.² A distinct advantage of this approach, relative to the traditional experiments in which atoms are subjected to intense laser pulses, is that the target can be tailored so as to optimize physical effects of interest. For instance, double-well structures in far-infrared fields appear to be well suited to the investigation of a mechanism for the generation of frequencies considerably higher than (and not necessarily harmonics of) the driving frequency at avoided crossings of quasienergies. There are also effects which have no counterpart in the atomic world. For example, as we have pointed out, the bandwidth of minibands in superlattices can collapse nearly to zero when the sample is interacting with laser radiation, which leads to the inhibition of wave-packet spreading. In both of these cases, measuring the frequency spectrum of the scattered radiation seems to provide a valuable tool for quasienergy spectroscopy in solid-state systems.

ACKNOWLEDGMENTS

We are grateful to Dr. S. J. Allen, Dr. Paulo Guimaraes, and Dr. Mark Sherwin, and to Brian Keay, for helpful discussions, particularly with regard to the experimental aspects of the problems discussed here. We thank Dr. Walter Kohn for several very useful conversations, including detailed discussion of Ref. 22, and Dr. Nguyen Hong Shon for bringing Ref. 25 to our attention. M.H. thanks Dr. G. Ahlers for kind hospitality at UCSB’s Center for Nonlinear Science. This work was supported in part by a research grant for the Alexander von Humboldt Foundation (M.H.) and by the National Science Foundation (D.H.) under Grant No. DMR-8906783.

- ¹See, e.g., C. Weisbuch and B. Vinter, *Quantum Semiconductor Structures* (Academic, San Diego, 1991).
- ²M. S. Sherwin, in *Quantum Chaos*, edited by G. Casati and B. V. Chirikov (Cambridge University Press, London, in press).
- ³B. Birnir, B. Galdrikian, R. Grauer, and M. S. Sherwin, *Phys. Rev. B* (to be published).
- ⁴F. Bloch, *Z. Phys.* **52**, 555 (1928).
- ⁵A. M. G. Floquet, *Ann. Ecole Norm. Sup.* **12**, 47 (1883).
- ⁶Ya. B. Zel'dovich, *Zh. Eksp. Teor. Fiz.* **51**, 1492 (1966) [*Sov. Phys. JETP* **24**, 1006 (1967)].
- ⁷V. I. Ritus, *Zh. Eksp. Teor. Fiz.* **51**, 1544 (1966) [*Sov. Phys. JETP* **24**, 1041 (1967)].
- ⁸H. Sambé, *Phys. Rev. A* **7**, 2203 (1973).
- ⁹J. S. Howland, *Ann. Inst. Henri Poincaré* **49**, 309 (1989).
- ¹⁰S. H. Autler and C. H. Townes, *Phys. Rev.* **100**, 703 (1955).
- ¹¹J. H. Shirley, *Phys. Rev.* **138**, B979 (1965).
- ¹²L. Allen and J. H. Eberly, *Optical Resonance and Two-Level Atoms* (Wiley, New York, 1975).
- ¹³See, e.g., C. P. Slichter, *Principles of Magnetic Resonance* (Harper & Row, New York, 1963).
- ¹⁴W. Bloss, D. Hone, and D. J. Scalapino, *Nucl. Phys. A* **314**, 436 (1979).
- ¹⁵I. I. Rabi, N. F. Ramsey, and J. Schwinger, *Rev. Mod. Phys.* **26**, 167 (1954).
- ¹⁶If the electromagnetic field is quantized, the counter-rotating terms can be eliminated formally by a suitable Bogoliubov transformation of the photon creation and destruction operators [C. Baxter, M. Babiker, and R. Loudon, *J. Mod. Opt.* **37**, 685 (1990)]. However, although this is useful for determining the ground state of the two-level system in a cavity, it is not helpful for the problem of interest here. The transformed Hamiltonian is formally simple, but the transformed Bose operators (linear combinations of photon creation and destruction operators) which appear there have no simple relation to the strong applied electric field.
- ¹⁷J. von Neumann and E. Wigner, *Phys. Z.* **30**, 467 (1929). Translated in R. S. Knox, A. Gold, *Symmetry in the Solid State* (Benjamin, New York, 1964).
- ¹⁸B. R. Mollow, *Phys. Rev.* **188**, 1969 (1969).
- ¹⁹J. Esaki and R. Tsu, *IBM J. Res. Dev.* **14**, 61 (1970).
- ²⁰We neglect Coulomb-interaction effects, including plasma oscillations and excitons, as is appropriate to the low electron density regime.
- ²¹J. M. Ziman, *Electrons and Phonons* (Oxford University Press, London, 1960), pp. 92–94.
- ²²W. Kohn, *Phys. Rev.* **115**, 1460 (1959).
- ²³The corrections to the adiabatic approximation are exponentially small in the ratio $\Delta/e\mathcal{E}_0a$ (with an additional numerical factor of order π^2), so that even modest ratios are adequate for this approximation to be valid.
- ²⁴L. I. Schiff, *Quantum Mechanics* (McGraw-Hill, New York, 1968), pp. 289–291.
- ²⁵D. H. Dunlap and V. M. Kenkre, *Phys. Rev. B* **34**, 3625 (1986).
- ²⁶F. Grossmann, T. Dittrich, P. Jung, and P. Hänggi, *Phys. Rev. Lett.* **67**, 516 (1991).
- ²⁷M. Holthaus, *Z. Phys. B* **89**, 251 (1992).
- ²⁸M. Holthaus, *Phys. Rev. Lett.* **69**, 351 (1992).
- ²⁹A. Rabinovitch and J. Zak, *Phys. Rev. B* **4**, 2358 (1971).
- ³⁰A. A. Ignatov and Yu. A. Romanov, *Phys. Status Solidi B* **73**, 327 (1976).